Analytical Solution of High β_p Equilibria with Natural Inboard Poloidal Null Configuration Obtained in the Spherical Tokamak QUEST*)

Kishore MISHRA[1)], Hideki ZUSHI[2)], Hiroshi IDEI[2)], Saya TASHIMA[1)], Santanu BANERJEE[1)], Makoto HASEGAWA[2)], Kazuaki HANADA[2)], Kazuo NAKAMURA[2)], Akihide FUJISAWA[2)], Yoshihiko NAGASHIMA[2)], Keisuke MATSUOKA[2)], Arseny KUZMIN[2)], Takumi ONCHI[2)] and QUEST Team

[1)]*IGSES, Kyushu University, Kasuga, Fukuoka 816-8580, Japan*
[2)]*RIAM, Kyushu University, Kasuga, Fukuoka 816-8580, Japan*

(Received 10 December 2013 / Accepted 22 April 2014)

High β_p ($\varepsilon\beta_p \sim 1$) equilibria obtained in a ECW heated Ohmic plasma is investigated using a simple analytic solution of Grad-Shafranov equation. The formation of a natural inboard poloidal null associated with high β_p is explained consistently by high diamagnetism and negative triangularity. As β_p is increased, the poloidal null point penetrates further into the vacuum vessel, which is qualitatively explained by the analytic model. Transition from inboard (high field side) limiter bound to the natural divertor configuration is associated with a reduction of the edge safety factor without appreciable enhancement of MHD activities. Such a scenario is also addressed successfully with the model.

Keywords: tokamak plasma equilibrium, Grad-Shafranov equation, high beta plasma, natural divertor

DOI: 10.1585/pfr.9.3402093

1. Introduction

Spherical Tokamak is an attractive choice for future fusion reactors for its ability to operate at high poloidal beta (β_p) value, thereby increasing the bootstrap current fraction. However, the maximum achievable β_p is limited by a so called equilibrium limit, where an Inboard Poloidal field Null (IPN) appears at the high field side of the vacuum vessel. To describe such high β_p equilibria and to study its stability properties, analytical solution to Grad-Shafranov equation (GSE) is often useful. Earlier work of Solov'ev [1] with a simple pressure and poloidal current profile is extended [2–4] by including more linear stream functions to describe high β_p configuration. The issue of β_p equilibrium limit has been addressed theoretically earlier [1–4]. Nevertheless, owing to the dearth of experimental demonstration of IPN configuration, comparison of such models with experimental data is far from adequate. The natural IPN configuration is first observed transiently in CDX-U and DIII-D during the current ramp-up and closed flux formation [5] phase, but no measurements are done. In TFTR [6], a null point appeared at the inboard side in high β_p plasma formed by ramping down the plasma current (I_p) in a NBI heated plasma. Such high β_p plasma production and sustainment required > 16 MW of NBI power and could not be achieved at higher I_p. IPN configuration has not been realized or sustained effectively in tokamaks to date, albeit adequate demonstration of high β_p plasma [7–9]. In this work, we present the experimental IPN configuration obtained rather easily and flexibly by creating an anisotropic pressure distribution of energetic electrons generated by injecting a modest power (< 100 kW) of Electron Cyclotron Waves (ECW) in the Ohmic plasma. Such high β_p (~ 4) plasma with IPN configuration is shown to be stable and various equilibrium and stability studies are performed using a simple analytic solution of GSE. The equilibrium flux functions obtained from the model are compared with the results obtained from the magnetic measurements. With the help of the model, plasma equilibrium is investigated as a function of plasma diamagnetism and triangularity and is compared with the experimental results for both the standard limiter and IPN configurations. Important MHD surface functions like safety factor and magnetic shear along with β_p are computed from the model and compared with the measurements.

Outline of the paper is as follows: experimental detail of the IPN plasma formation is discussed next. Analytical solution of GSE is formulated in section 3. Section 4 provides an account of the computation of β_p from the analytic model and the variation of β_p with plasma triangularity and the null position. Finally, some conclusions are drawn in section 5.

author's e-mail: mishra@triam.kyushu-u.ac.jp

*) This article is based on the presentation at the 23rd International Toki Conference (ITC23).

2. High β_p IPN Plasma Formation in QUEST

QUEST is a medium sized spherical tokamak [10] with the major and minor radii of 0.68 and 0.4 m, respectively. The center stack (CS), which holds the Ohmic (OH) coil has an outer diameter of 0.2 m and the outer wall of the vacuum vessel is at 1.4 m with the flat divertor plates at $z \sim \pm 1$ m from the mid-plane. Inboard plasma boundary is defined by a limiter on the CS at 0.23 m. In the present experiment, I_p is initiated by injecting $\sim$ 100 kW of ECW power at 8.2 GHz for 150 ms from the two antennae located at the Low Field Side (LFS) followed by the OH phase. In the OH phase, I_p is fed back to the OH coil power supply in order to maintain it at -30 kA $\pm$ 10%. Here the negative I_p is defined clockwise as seen from the top of the torus. The toroidal field (B_t) is set at 0.29 T at the fundamental resonance $R_{fce} = 0.33$ m, where a vertical magnetic field $B_z \sim 25$ mT is applied. At 2 s of the I_p flattop, another ECW pulse is injected. This results an increase in I_p from -30 kA to -32 kA in 0.3 s (Fig. 1 (a)). Due to the feedback circuit, OH coil current is reversed transiently to produce a retarding electric field (positive loop voltage V_L) in order to bring back I_p to the feedback value. Plasma shape and position are identified by the magnetic measurements from the 64 flux loops outside the plasma. The magnetic flux contours are reconstructed by a fitting procedure described in ref. 11 and are shown in Fig. 1 (b). It can be seen that plasma configuration is changed from an inboard limiter (IL) during OH phase to IPN in the ECW phase. A tangentially viewing visible camera image also confirms

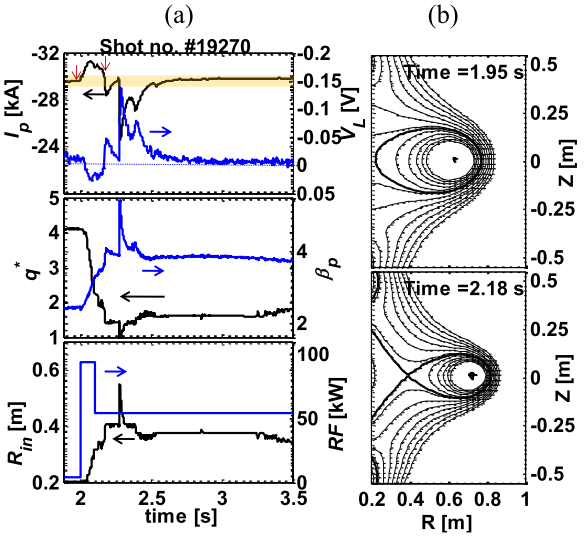

Fig. 1 Time traces of plasma current (I_p), one turn loop voltage (V_L), kink safety factor (q^*). The transient spike in β_p at $\sim$2.3 s is due to a minor disruption in I_p. The inboard plasma position (R_{in}) depicts separatrix formation ($R_{in} >$ 0.22 m) as β_p increased with ECW injection. Magnetic flux contours during OH phase (1.95 s) and ECW phase (2.18 s) show the formation of IPN configuration.

such transition in configuration, where the separatrix strike points on the limiter are clearly seen. The poloidal magnetic null point (R_{in}) measured by the flux loops is shown in Fig. 1 (a), which distinctly shows that it has moved inside the vacuum vessel up to 0.4 m in the ECW phase. The natural appearance of such inboard null is a consequence of high β_p formation. We evaluate β_p from the generalized Shafranov equation for radial force balance for the equilibrium vertical magnetic field [12]

$$B_z = \frac{\epsilon B_\theta(a)}{2}\left[ln\frac{8R_0}{a} + \beta_p + \frac{l_i}{2} - \frac{3}{2}\right], \quad (1)$$

where $B_\theta(a) = \mu_0 I_p/2\pi a$ is the poloidal magnetic field at the boundary $r = a$. l_i is the internal inductance assumed here to be unity and not varying.

The IPN plasma has an aspect ratio $A = R_0/a \sim 1.7$ to 2.6, hence equation (1) is deemed valid to describe the present equilibria in particular. β_p evaluated in this method shows an increment from 2.4 in OH phase to $\sim$ 4 in the ECW phase in $<$ 0.18 s. In order to maintain this high β_p plasma in equilibrium, B_z is increased from 26 mT in the OH phase to 33 mT during the ECW phase, or else I_p is not sustained. Requirement of high B_z is also evident from the fact that, the increased pressure gradient ($\nabla p = \boldsymbol{j} \times \boldsymbol{B}$) needs to be balanced by enhancing $\boldsymbol{B}$ at a fixed I_p.

It can be noted here that such high β_p plasma is stable from 2.5 - 3.5 s and there are no observable MHD instabilities. The kink safety factor $q* = \pi\varepsilon a(1+\kappa^2)B_0/\mu_0 I_p$ from the measurements shows that it is reduced from 4.1 (limiter) to 1.6 in the IPN configuration (Fig. 1 (a)). This is due to the reduction of plasma minor radius a, larger R_0 and reduced B_0 due to the shift of the plasma outward.

3. Analytic Solution of IPN Equilibria

For toroidal axisymmetric equilibria (independent of toroidal angle φ) magnetic field can be represented by $\boldsymbol{B} = (1/R)\nabla\psi\times\boldsymbol{e}_\varphi + B_\varphi\nabla_\varphi$, where ψ is the poloidal magnetic flux function, a constant on nested magnetic surfaces, φ is the toroidal angle of (R, Z, φ) cylindrical co-ordinate system and $\boldsymbol{e}_\varphi$ is unit vector along φ. Defining $G(\psi)$ as the poloidal current function so as to generate $B_\varphi = \mu_0 G/2\pi R$, GSE for such equilibrium can be expressed as,

$$R\frac{\partial}{\partial R}\left(\frac{1}{R}\frac{\partial\psi}{\partial R}\right) + \frac{\partial^2\psi}{\partial Z^2} = -\mu_0^2 G\frac{\partial G}{\partial\psi} - \mu_0(2\pi R)^2\frac{\partial p}{\partial\psi}. \quad (2)$$

GSE, in general needs to be solved numerically because of its non-linearity. However, a number of powerful yet simpler models to solve GSE analytically are described in refs. [1–3] and they have their inherent ability to choose geometrical parameters independently. We have here used the analytical solution discussed in ref. 2 for the spherical torus plasma equilibrium in particular, given as

$$\psi(R,Z) = \frac{c_0}{8}\frac{\sigma^2}{(1+\sigma^2)}\left[(R^2 - R_a^2)^2 + 4\frac{Z^2}{\sigma^2}(R^2 - \omega R_a^2) - 2\tau R_a^2\left(R^2\ln\frac{R^2}{R_a^2} - R^2 + R_a^2\right)\right], \quad (3)$$

where c_0 is related to pressure gradient, R_a represents magnetic axis and ω, σ are functions of plasma geometrical parameters through some complex functions of plasma diamagnetism factor τ. The factor τ is particularly important in spherical torus high beta plasma equilibria. For τ set to zero, equation (3) is reduced to Solov'ev plasma equilibrium solution. Although plasma diamagnetism and plasma shape, especially plasma triangularity, are coupled with each other, but the solution given above allows to choose the two parameters independently. Defining the plasma boundary value of poloidal flux as $\psi_b = (c_0/8)[\sigma^2/(1+\sigma^2)]R_b^4$, where R_b is a constant, the normalized poloidal magnetic flux function can be defined as,

$$\psi R,Z = \frac{\psi_b}{R_b^4}\left[(R^2-R_a^2)^2 + 4\frac{Z^2}{\sigma^2}(R^2-\omega R_a^2) - 2\tau R_a^2\left(R^2\ln\frac{R^2}{R_a^2} - R^2 + R_a^2\right)\right]. \quad (4)$$

The constants in the above equation can be expressed as functions of plasma geometrical parameters like, inverse aspect ratio ε, elongation k, triangularity δ [2].

$$\frac{R_a}{R_b} = f(\varepsilon,\tau,R_0), \omega = g(\tau,\varepsilon,\sigma,R_a,R_b), \quad \sigma = h(\kappa,\varepsilon,\sigma,\tau,R_a). \quad (5)$$

Here τ and c_0 are chosen iteratively such that the imposed boundary condition is satisfied while constraining the parallel surface current $\lambda(\psi) = \mu_0(GI' - IG')/(qG - I)$, at $\psi = \psi_b$ to zero. Here, both I (toroidal current) and q (safety factor profile) are flux functions and the prime denotes differentiation with respect to the flux function. All these functions are obtained from the two basic surface functions $U(\psi)$ and $V(\psi)$ evaluated by numerical integration as described in ref. [2].

In ref. 2, no constraint on I_p is imposed and it is calculated self consistently. However in the present case we have forced the total I_p bounded by $\psi = \psi_b$ to be fixed and is set to the measured I_p in addition to the $\lambda(\psi_b) = 0$ boundary condition. By doing so we could choose the constant c_0 corresponding to the actual I_p. This simplified the iteration procedure and one only needed to find the optimum τ so as to satisfy the boundary condition. The plasma geometrical parameters ε, k, δ, R_0 inferred from the magnetic measurements, I_p measured from the Rogowsky coil and the applied toroidal magnetic field B_0 are given as the input parameters to the model. $\psi(R,Z)$ are the output of the model, which are used to find boundary flux contour as defined by the inner limiter. Such boundary flux contours computed from the model are superimposed on the LCFS inferred from the magnetic measurements, and are shown in Fig. 2. It is seen that the analytic solution agrees excellently with the flux loop reconstruction. It is also important to correctly choose τ as it has a direct bearing on the resulting β_p and plasma boundary. For a critical value of τ, a field null just appears inside the vessel, which is the limiting β_p for IL to IPN transition as discussed in the next section. However, the equilibria shown below at 1.95 s is perfectly in IL configuration.

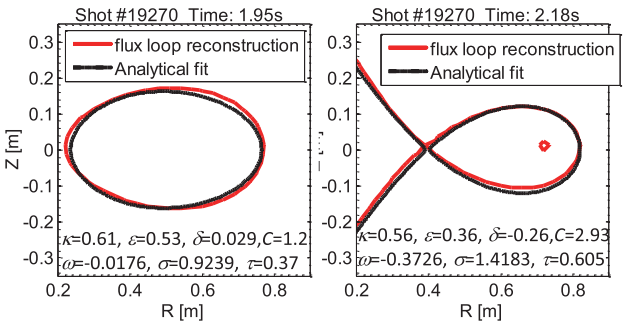

Fig. 2 Boundary flux contours for IL and IPN plasma are compared from the analytic model and the flux loop reconstruction. The model parameters for both the cases are inscribed.

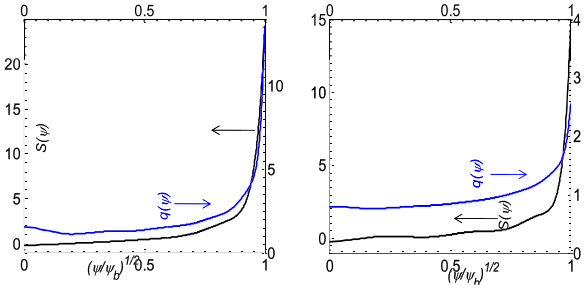

Fig. 3 Magnetic shear (S) and safety factor (q) as flux functions computed from the analytic model: left is limiter plasma; right is for IPN plasma.

Once a convergence of the solution is found at the boundary, it is easy to find various flux functions like magnetic well, magnetic shear $S(\psi)$, safety factor $q(\psi)$ etc. In Fig. 3, S and q for the two configurations (IL and IPN) are shown. From $q(\psi)$ profile it is seen that q_{95} is reduced from 4.3 in IL to 1.5 in the IPN configuration and such reduction of q_{95} during the IPN formation is consistent with the measured q^* as shown in the Fig. 1. The central q (see Fig. 3) for the IPN plasma is marginally below 1. Absence of any confirmed sawteeth oscillations in these discharges, however, suggests that central q may not be below 1. Considering ECW heating in low density plasma ($n_{e\_ave} < 8\times10^{17}$ m^{-3}), strong pressure anisotropy ($p_\perp \gg p$) is expected. The analytic solution presented here however, assumes an isotropic pressure profile. It has been shown earlier [13] that the estimation of central q can be significantly underestimated by this assumption. The role of pressure anisotropy in the present equilibrium is left as a future work.

4. Poloidal Beta

Computation of β_p from the analytic model is quite intriguing, particularly in IPN plasma. The hunting for op-

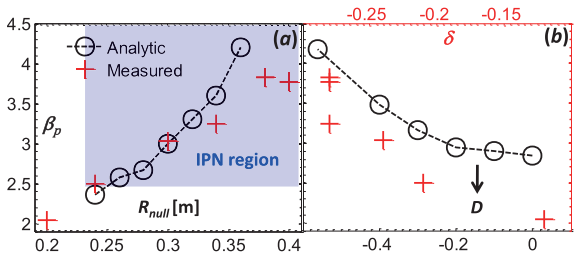

Fig. 4 Poloidal beta (β_p) computed from the analytic solution (circles) and magnetic measurements (cross) as a function of null position (R_{null}) and triangularity. D is the triangularity parameter in the analytic model and δ is the measured plasma triangularity. The values of model parameters for different points are chosen to best match the LCFS, $E = 0.85$ - 1.43, $D = 0$ to -0.56, $H = H_c$.

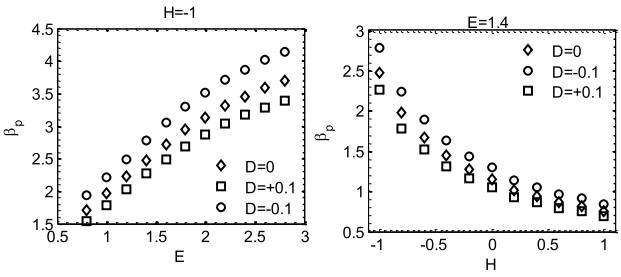

Fig. 5 Poloidal beta (β_p) computed from the analytic solution as a function of E and H for different D parameters at fixed $R_{null} = 0.3$ m. Higher elongation, diamagnetism and negative triangularity, all are favorable for increasing β_p.

timum τ corresponding to $\lambda(\psi_b)$ minimum is often cumbersome in the method described in the previous section. Additionally from Fig. 1 it is seen that as β_p increases beyond 2.5 with application of ECW, R_{null} ($= R_{in}$) moves in to the vacuum vessel and has a very good correlation with β_p. So to study the IPN plasma and relation of β_p with R_{null} more easily, we dwelt on the treatment described in the ref. 3, where IPN equilibria can be studied more flexibly by introducing the following transformations

$$D = \frac{\omega}{1-\omega},\ E = \frac{\sigma}{\sqrt{1-\omega}} \text{ and } H = -2\tau, \qquad (6)$$

where, D represents plasma triangularity, E relates to plasma elongation and H is related to diamagnetism. The analytical GSE in this case is same as eq. 4. As H is increased, a poloidal field null appeared at the high field side. Correspondingly the critical H is defined as a function of R_{null} as $H_c = 2(1 - R_{null}^2)/\ln R_{null}^2$, where the null point just about to appear. This introduces much flexibility in computing boundary flux functions including the poloidal magnetic field. $\beta_p = 2\mu_0\langle P\rangle_v/\langle B_p\rangle^2$ is calculated as described in ref. 3. In Fig. 4 we have computed β_p as a function of R_{null} and D from the analytic model for various IPN equilibria corresponding to $H = H_c$ to reproduce high β_p configurations. β_p shows an increasing trend both with larger R_{null} position and higher negative values of D for the range of $E = 0.85$ - 1.43. This prediction is consistent with the measured values of β_p as shown in the Fig. 4 at discrete time intervals. Figure 4 (a) shows a critical $\beta_p^c \sim 2.5$ at which the IL-IPN transition occurs and is supported by the model. In Fig. 5 we show the variation of β_p as a function of E and H for different D values. It shows that β_p can be increased with higher elongation (E) and larger negative triangularity. It also shows that for higher diamagnetic factor (H), β_p is increased. Plasma boundary is largely decided by the choice of these parameters, however, in all these cases, at a critical H_c or higher negative triangularity, IPN configuration is achieved for $\beta_p^c >\sim 2.5$. In some cases, IPN configuration is also achieved at a marginally lower $\beta_p < \beta_p^c$ if $H > H_c$. However, such a scenario is not obtained in the present experiment. The boundary solutions obtained in the analytic model satisfying the high β_p configuration (Fig. 4) are found to be for $\kappa \sim 1$, which is higher than the fitted boundary obtained from the magnetic measurements ($0.6 < \kappa < 0.7$). This difference can be attributed to the consideration of simple isotropic pressure profile or the choice of current profile, which requires further study. However, the simple analytic solution can qualitatively explain the equilibrium characteristics of high β_p IPN plasma configurations obtained in our experiment.

5. Conclusion

High β_p equilibrium is obtained in a ECW heated OH target plasma in QUEST. With high β_p, plasma configuration is transformed from an inboard limiter to inboard natural divertor with a poloidal field null appearing at the inboard side. A simple analytic solution is demonstrated to explain this phenomenon, which agrees well with the measurements. This further defines a critical β_p for the transition from IL to IPN. The model also shows that β_p increases with a higher value of negative triangularity, consistent with the measurements and predicts that β_p can be raised by suitable shaping of plasma to have a negative triangularity. The reduced q with IPN formation is also consistent with the analytic model prediction. However the apparent low value of central q indicated by the present model may need to be revisited by including anisotropic pressure in the model.

Acknowledgement

This work is supported by Grant-in-aid for Scientific Research (S24226020, A21246139). This work is also performed with the support and under the auspices of the NIFS Collaboration Research Program (NIFS11KUTR06 3).

[1] L.S. Solov'ev, Sov. Phys. JETP **26**, 400 (1968).
[2] R.H. Weening, Phys. Plasmas **7**, 3654 (2000).
[3] B. Shi, Phys. Plasmas **12**, 122504-1 (2005).
[4] A.J. Cerfon and J.P. Friedberg, Phys. Plasmas **17**, 032502 (2010).

[5] C.B. Forest *et al.*, Phys. Plasmas **1**, 1568 (1994).
[6] S.A. Sabbagh *et al.*, Phys. Fluids **B3**, 2277 (1991).
[7] T.C. Simonen *et al.*, Phy. Rev. Lett. **61**, 1720 (1988).
[8] S.C. Luckhardt *et al.*, Phy. Rev. Lett. **62**, 1508 (1989).
[9] T. Maekawa *et al.*, Nucl. Fusion **31**, 1394 (1991).
[10] K. Hanada *et al.*, Plasma Fusion Res. **5**, S1007 (2010).
[11] M. Hasegawa *et al.*, IEEJ Trans. FM **132**, 477 (2012).
[12] J.P. Freidberg, *Ideal Magnetohydrodynamics* (Plenum Press, New York, 1987).
[13] W. Zwingmann, L-G Eriksson and P. Stubberfield, Plasma Phy. Control. Fusion **43**, 1441 (2001).